Electronic Supplementary Material (ESI) for Physical Chemistry Chemical Physics.

Supporting Information

Model of Protocell Compartments - Dodecyl Hydrogen Sulfate Vesicles†

Bin Liu,[1] Meihua Gao,[1] Haiping Li, [2] Jianqiang Liu,[3] Shiling Yuan,[1] Na Du, [1]* Wanguo Hou,[1]

[1] Key Laboratory of Colloid and Interface Chemistry (Ministry of Education), Shandong University, Jinan 250100, P.R. China;

[2] National Engineering Technology Research Center for Colloidal Materials, Shandong University, Jinan 250100, P.R. China.

[3] School of Physics, Shandong University, Jinan 250100, PR China.

Experimental details

Synthesis of dodecyl hydrogen sulfate (DHS)

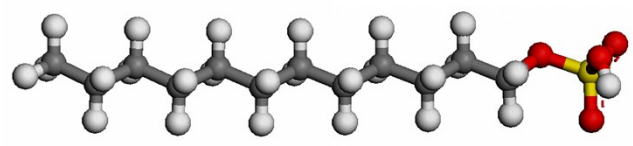

Scheme S1. Molecular structure model of dodecyl hydrogen sulfate ($C_{12}H_{25}SO_4H$). The atom coloring scheme is C, gray; O, red; S, yellow; H, white.

Dodecyl hydrogen sulfate (**Scheme S1**), noted as DHS, was prepared by mixing of sodium dodecyl sulfate (SDS, >99% Sigma) saturated aqueous solution (150 $g \cdot L^{-1}$) and a molar equivalent of concentrated hydrochloric acid.[1, 2] The DHS was extracted into chloroform 8 times. And then the organic solvents were removed through a rotary evaporation at 30 ^oC. The residual water was removed by freeze-drying technology. Finally, the recovered white powder was ground in the agate mortar before use and the product yields were about 43.3%. The molecular structure of the obtained DHS was characterized by NMR (**Figure S1**). Particularly, the active hydrogen of DHS molecule was confirmed by the disappearing of the active H peak after the addition of D_2O (99.96%, Sigma) to the NMR sample.

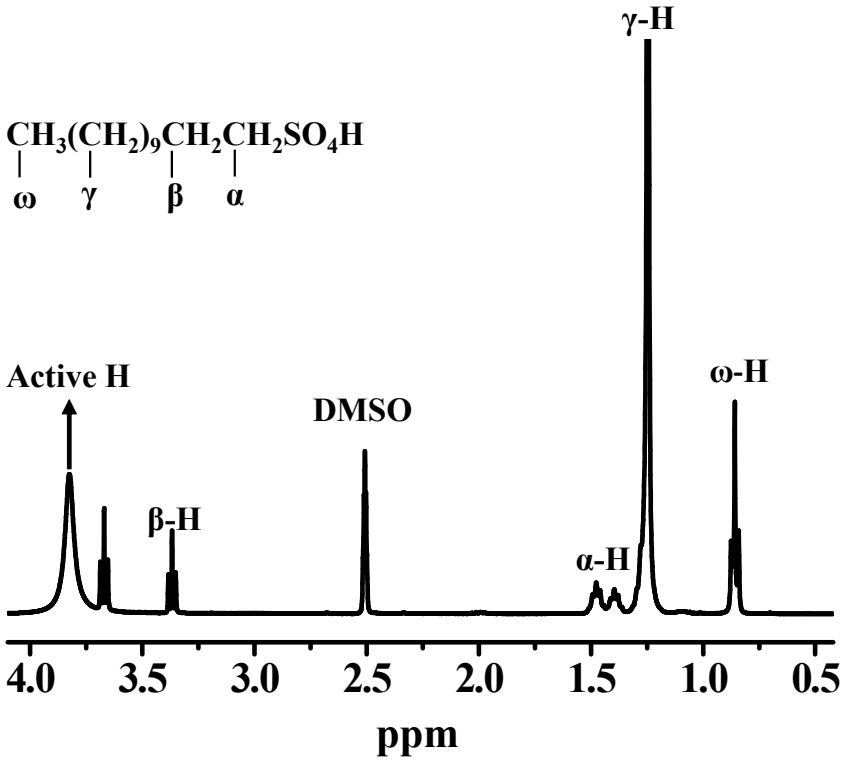

Figure S1. [1]HNMR spectra of DHS in DMSO-d_6. After the addition of D_2O to the NMR sample, the peak of active hydrogen disappeared in the spectra.

Preparation of DHS vesicles

The vesicular solution of DHS was prepared in pure water by dissolving a weighed amount of DHS and sonicated until dissolved to obtain samples of different concentrations. The DHS solutions were kept in thermodynamic bath at 25 ± 0.5 °C for at least 72 h before measurements. Ultrapure water with a resistivity of 18.2 MΩ·cm was obtained using a Hitech-Kflow water purification system (Hitech, China).

Reproduction of DHS vesicles

DHS vesicles solutions (8 mM) were prepared with 0.1 M citric acid-sodium citrate buffer solution (pH = 3.0). For experiments designed to follow the kinetic growth and division of vesicles, six equiv of SDS micelles were added into DHS vesicles solutions. Samples of

intermediate transition were collected at different time intervals after the addition of micelles and characterized by TEM, LSCM, AFM and DLS.

Characterization of Samples

Nuclear magnetic resonance (NMR) Spectroscopy. ^{1}H NMR spectra were recorded at 25.0 ± 0.1 °C on a Brüker Advance 400 spectrometer (Brüker, Switzerland) equipped with a pulse field gradient module (Z-axis), using a 5 mm BBO probe at a frequency of 400.13 MHz. Samples for ^{1}H NMR were prepared in DMSO-d_6 (99%, Sigma).

pH Titration. The pH titration method[3, 4] was employed to determine the apparent pK_a value of DHS at 25±0.5 ^{o}C. A DHS solution (5 mM, 20 mL) was titrated with a 0.1 M NaOH solution under a nitrogen atmosphere, and the change in pH of the solution was monitored using a FE20 pH meter (Mettler Toledo, Sweden). The apparent pK_a value was calculated by employing the Henderson-Hasselbach equation, pH = pK_a + log ([A$^-$]/[HA]). It relates pH and pK_a to the equilibrium concentrations of dissociated acid [A$^-$] and non-dissociated acid [HA] respectively. The inflection point of pH titration curves is commonly thought to be related to the complete ionization of acid. And the pH value at 50% of the ionization volume ([A$^-$]=[HA]) corresponds to the pK_a of the acid. Thus, the apparent pK_a was calculated as the pH of the solution at half the neutralization volume (**Figure S5**). To obtain accurate apparent pK_a value, three titrations were performed and mean apparent pK_a value was calculated to be 3.11.

Cryogenic (Cryo-) TEM Observations. The morphology of the aggregates in solution was observed by cryo-TEM. The samples were prepared in a controlled environment vitrification system (Cryoplunge TM3, USA) at 25 ^{o}C and 95% relative humidity. A 4.0 μL aliquot of sample solution was loaded onto a carbon-coated copper grid. The excess solution was then

blotted off with filter paper, producing a thin film suspended on the mesh holes. After ca. 10 s, the sample-loaded grid was quickly immersed in liquid ethane and cooled with liquid nitrogen. The vitrified sample was transferred to a cryogenic specimen holder (Gatan 626) and examined on a JEM-1400 TEM (JEOL, Japan) at an accelerating voltage of 120 kV.

Negative-Staining (NS) TEM Observations. NS-TEM images were recorded on a JEM-1011 TEM (JEOL, Japan) operating at an accelerating voltage of 100 kV. A drop of sample solution was loaded onto a 300-mesh carbon coated copper grid and allowed to stand for 30 s. The excess solution was blotted off with filter paper, followed by staining with uranyl acetate solution (5 μL, 1% w/v). The specimens were kept in a desiccator overnight before observation.

Freeze-Fracture (FF) TEM Observations. Fracturing and replication were carried out in a Balzers BAF-400D high-vacuum freeze-etching system (Leica, Germany). A small amount of sample was dropped on the specimen carrier and was inserted rapidly into the liquid ethane at -175 ^{o}C which was cooled with liquid nitrogen. After that, under conditions of -175 ^{o}C and 10^{-7} Pa, samples were fractured and replicated by using the Leica EM BAF 060 equipment. Pt/C at 45° and C at 90° were sprayed onto the fracture surface forming a 2.5 nm thick film and 18 nm thick film, respectively. The replicas were observed with a JEM-1011 TEM (JEOL, Japan) operating at an accelerating voltage of 100 kV.

Scanning Electron Microscope (SEM) Observations. SEM images were recorded on a Gemini SEM 300 (Zeiss, Germany). Samples for SEM measurement (on a 300-mesh carbon coated copper grid) were sputtered with a 5 nm thick platinum coating.

Dynamic Light Scattering (DLS) Measurements. DLS was carried out at scattering angle of 90°. A standard laser light scattering spectrometer (Brookhaven, England) equipped with a coherent radiation 200 mW diode pumped solid-state 488 nm laser and a Brookhaven Instruments Corporation (BI-9000AT) correlator were used for the measurements. The obtained data were analyzed by CONTIN.[5]

Differential Scanning Calorimetry (DSC) Measurements. DSC measurements were performed on a DSC8500 calorimeter (PerkinElmer, USA) over the temperature range of −10 ~ 100 °C at a scan rate of 0.5 °C·min^{-1}. The samples were measured in aluminum pans under the nitrogen flow and an empty aluminum pan was used as a reference.

Equilibrium surface tension. Equilibrium surface tension (g) measurements were performed on a JYW-200B tensiometer (Chengde Dahua Instrument Co., Ltd, China) using the ring method. Prior to measurements, all test solutions were equilibrated for at least 10 min. The γ value for each measurement was taken after the change in the observed value was less than 0.1 mN·m^{-1}. The temperature of the measurement cell was controlled at 25.0 ± 0.1 °C using a thermostatic bath. Three measurements were performed for each sample, and the average value was reported.

Transmittance (T_r) Measurements. An ultraviolet-visible (UV-vis) spectrometer (Hewlett-Packard 8453, Germany) was employed for T_r measurements, at 25 ± 0.5 °C and a wavelength of 400 nm. Sample was placed in a cell covered with a plastic cap to prevent evaporation. The reference solution is water.

Steady State Fluorescence Measurements. The steady state fluorescence measurements were performed on a fluorescence spectrophotometer (Hitachi F-7000, Japan) with a 150 W Xe lamp. The fluorescence emission spectra of pyrene probe (1.0 μM, Aladdin) in DHS solution were recorded between 350 nm and 550 nm by excitation at 335 nm, using excitation and emission slit widths of 5 and 2.5 nm, respectively. The fluorescence emission spectra of nile red (2.5 mg/L, Aladdin) in DHS solution were recorded between 550 nm and 800 nm by excitation at 530 nm, a scan rate of 1200 nm/min, using excitation and emission slit widths of 10 and 10 nm, respectively. All measurements were taken at 25 ± 0.5°C.

Conductivity Measurements. Conductivity (κ) measurements were performed on a DSJ-308A digital conductivity meter (Shanghai REX Instrument Factory, China) with a DJS-1C

glass electrode. The temperature of the measurement cell was controlled at 25±0.1 °C by a thermostatic bath. The tests were performed in triplicate, and the final values are the average of the three measurements. For the ions (K^+ and Cl^-) entrapment experiment (**Figure S10**), 50 μL (500 mM) KCl solution was added into DHS solutions under different concentrations (10 mL). All the solutions (KCl solution, DHS solution, and KCl in DHS solution) were left for 6 h for equilibration before measurement, and the conductivity values of them were noted as κ (DHS), κ (KCl), and κ (DHS + KCl), separately. The variation of conductivity ($\Delta\kappa$) is deduced from the following equation:

$$\Delta\kappa = \kappa\,(\mathrm{DHS}) + \kappa\,(\mathrm{KCl}) - \kappa\,(\mathrm{DHS + KCl})$$

The tests were performed in triplicate, and the final values are the average of the three measurements.

Atomic Force Microscope (AFM) Observations. A Nanoscope IIIa Multimode AFM (Digital Instruments Corp., USA) was used to examine the morphology of the aggregates in solutions deposited on mica wafers. AFM images were acquired in tapping mode using a Si tip cantilever with a force constant of 40 $N \cdot m^{-1}$.

Laser scanning confocal microscopy (LSCM). Images were recorded on an Olympus IX81 fluorescence microscope (Olympus Optical Co., Ltd, Japan). 10 μL of an aqueous solution of Nile red (M_w = 318.38 $g \cdot mol^{-1}$; 0.01 $mg \cdot mL^{-1}$; TCI), calcein (M_w = 622.53 $g \cdot mol^{-1}$; 0.01 $mg \cdot mL^{-1}$; Sigma), or FITC-BSA (66 KD; 0.05 $mg \cdot mL^{-1}$; X-Y Biotech) was added to 100 μL DHS solutions (8 mM), where the optical excitations were carried out with 488 nm, 445 nm, 490 nm argon laser beam, and fluorescence emissions were detected over a range of 560−630 nm, 470−610 nm, 520−530 nm, separately. The uptake or exclusion of the solutes was monitored by fluorescence microscopy.

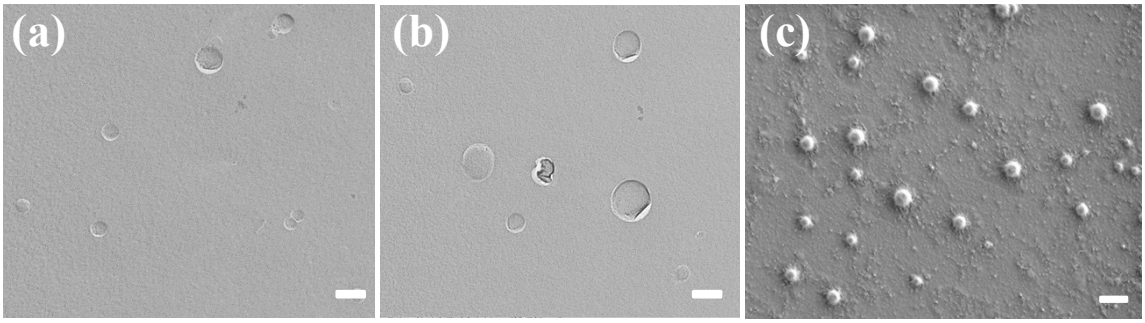

Figure S2. (a and b) Freeze-fracture TEM images and (c) SEM image of DHS solution at 5 mM, 25 °C, Scale bar: 200 nm.

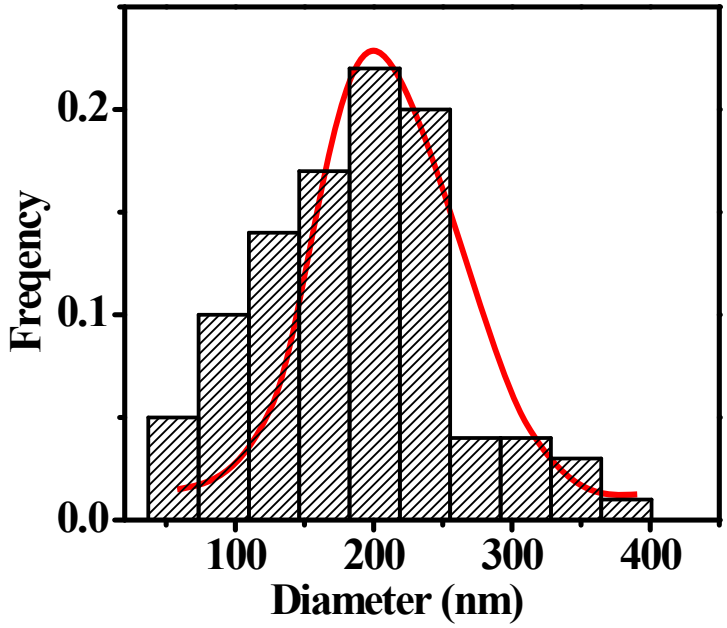

Figure S3. Vesicle size distribution histogram calculated from the TEM observation at DHS concentration of 5 mM at 25 °C. The size distribution peak centers around 200 nm. (counts = 100, the data refer to cryo-TEM observation)

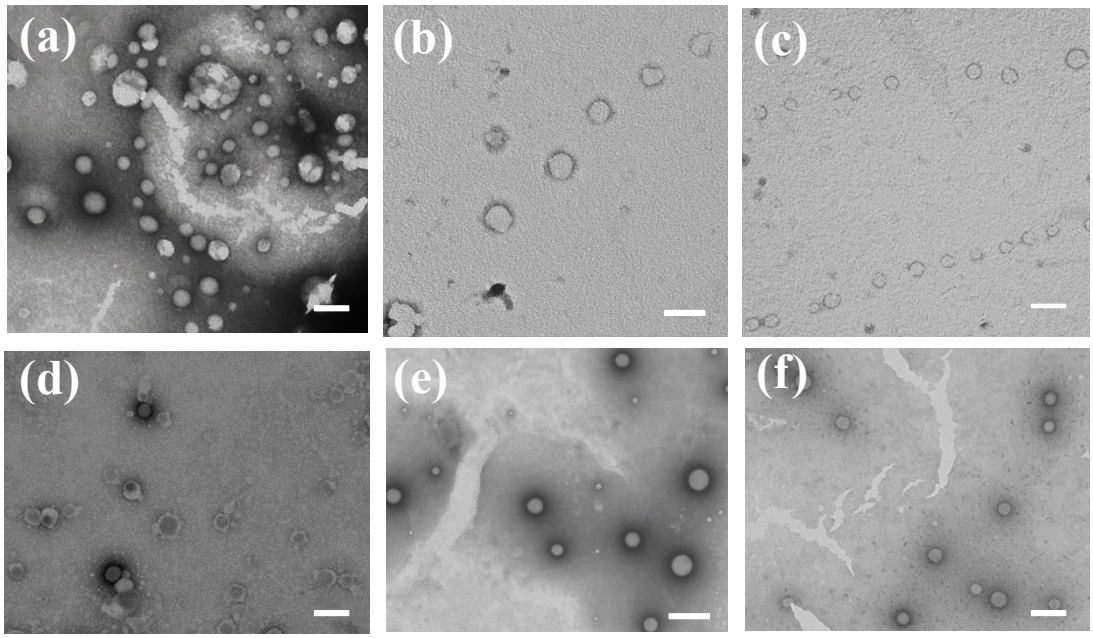

Figure S4. Negative-staining TEM images of DHS solution at concentration of (a, d) 0.5 mM, and (b, c, e, f) 2 mM after (a-c) standing 14 days and (d-f) six months at 25 ± 0.5 °C. It shows that the DHS vesicle phase could exist even in very diluted solutions and have good time stabilities at room temperature. Scale bar: 200 nm

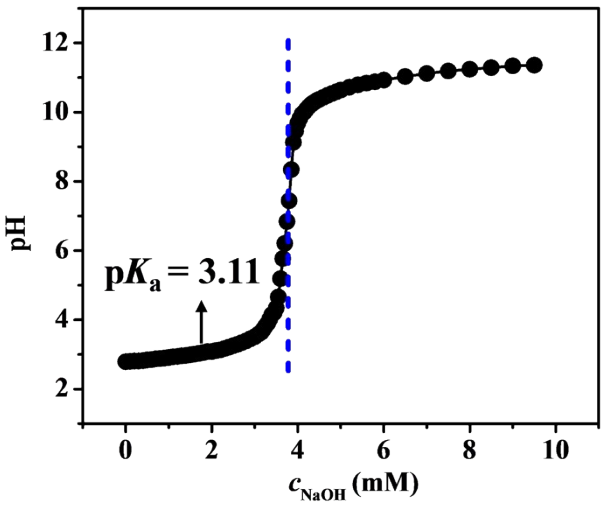

Figure S5. pH titration curve of DHS solution (5 mM) at 25 °C. The inflection points of pH titration curves are commonly thought to correspond to the complete ionization of acidic surfactants, and the pH values at half the ionization volume are defined as the apparent pK_a of the surfactant. Three titrations were performed and mean apparent pK_a value (3.11 in this case) was calculated. The deviation of the experimental equivalence point from the ideal equivalence point might due to the presence of impurities in the synthesized DHS sample.

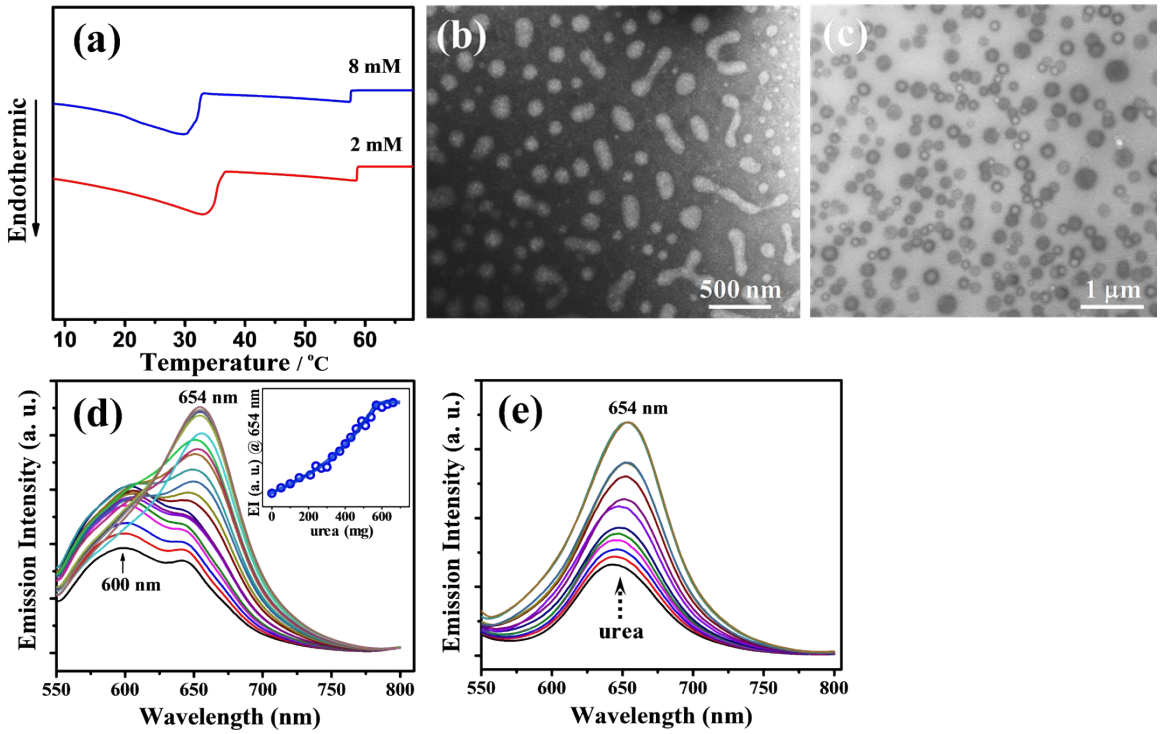

Figure S6. (a) DSC traces for DHS aqueous solutions at different concentrations. The peak around 30-35 °C might correspond to the phase transition of vesicles with different shapes. The minimal endothermic peak (58 °C) might indicate the disruption of H-bonding within $C_{12}H_{25}SO_4H$-$C_{12}H_{25}SO_4^-$ dimers. (b) NS-TEM images of DHS solutions (8 mM) at 35 °C. Elongated vesicles are observed. (c) NS-TEM images of DHS solutions (8 mM) recovered from 35 °C and placed back to 25 °C. Spherical vesicles are observed. (d) Effect of urea addition on the emission spectra (λ_{ex} = 530 nm) of Nile red encapsulated in DHS vesicles. The emission peaks at 600 nm correspond to the Nile red molecules encapsulated between the hydrophobic bilayers of vesicles. The gradual addition of urea to a Nile-red-encapsulated (hydrophobic guest) vesicle solution resulted in the appearance of a new emission peak at 654 nm, which was where the emission band appeared for Nile red in bulk water.[6] The emission intensity at 654 nm was plotted (inset) as a function of urea, which revealed the complete release in the presence of 570 mg of urea. (e) Emission spectra of Nile red in the presence of different concentration of urea in water. The emission intensity of hydrophobic Nile red in aqueous medium increased with the addition of urea. It is might attributed to non-specific interactions of the dye with urea, which lead to the red shift of the emission peaks at the same time. Similar results had been reported in the Ref 32 of article.

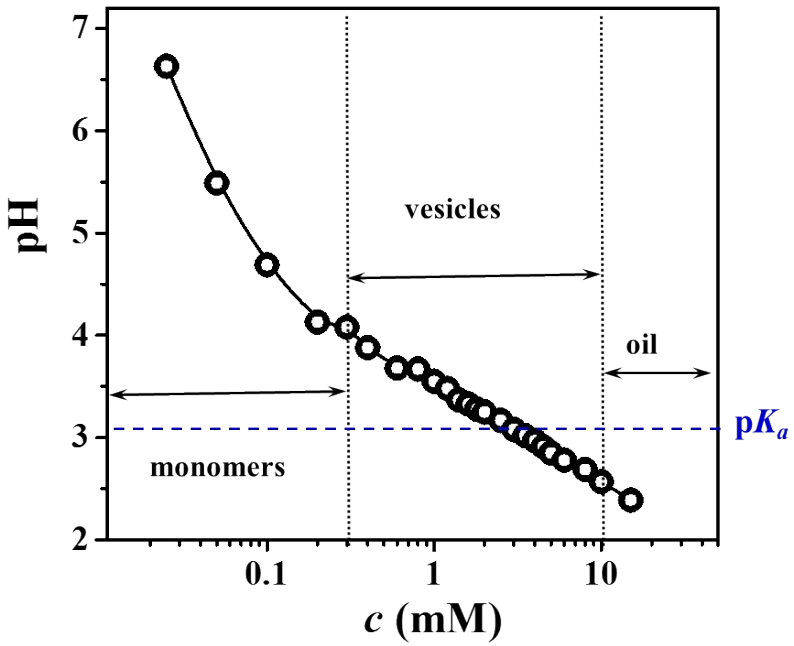

Figure S7. The variation of pH value at different DHS concentrations at 25 °C. The regions for the presence of monomers, vesicles and oil droplets are observed or deduced by optical microscope, TEM, DLS and eyes. DHS vesicle phase forms nearby pH 3.11 (apparent pK_a).

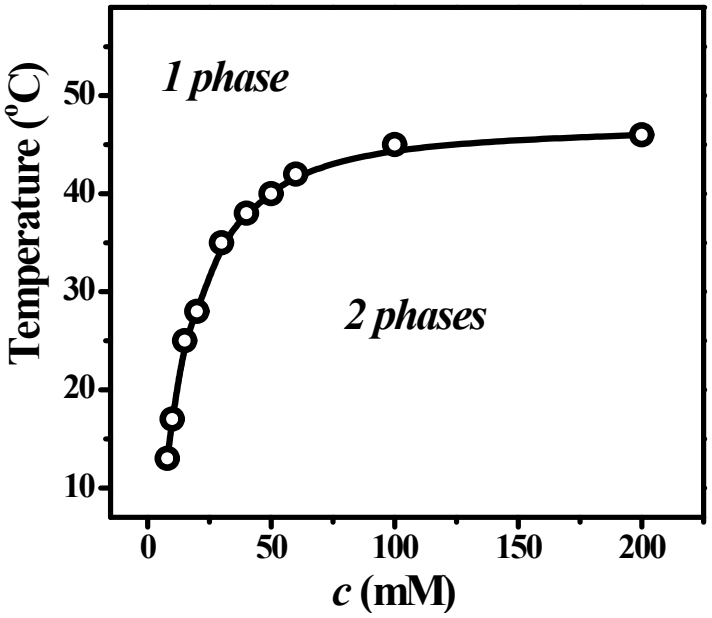

Figure S8. Solubility curve of DHS in water. The solubility limit of DHS is 10 mM at 25 °C. The data are collected in the system without buffering, and the pH values of each point were given in Fig. S7.

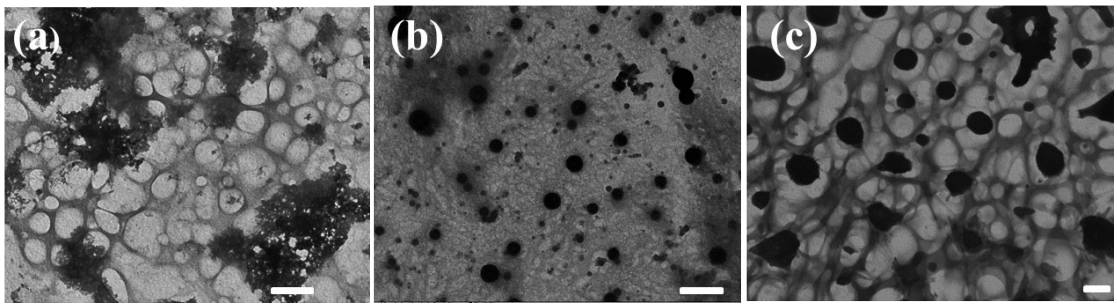

Figure S9. NS-TEM images of vesicles coexist with oil droplets at different concentration of DHS at 25 °C. (a) 20 mM, (b) 50 mM, and (c) 100 mM. Oil droplets appear from the aqueous phase at room temperature when the concentration of DHS is more than 10 mM, the size of oil droplets grow larger upon the increase of DHS concentration. Probably this is due to pH decrease as the DHS concentration increase, and thus by the reduction of ionization. Scale bar: 1 μm.

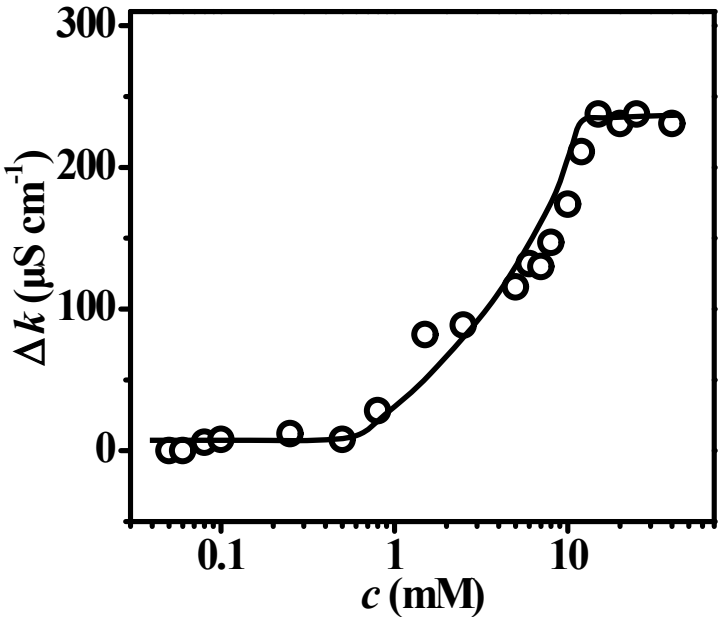

Figure S10. The variation of the conductivity change (Δκ) with DHS concentration in aqueous solution (c_{KCl} =2.5 mM). Since the vesicles are able to entrap a part of the solvent and the salt, they prevent the entrapped charge carriers (K^+ and Cl^- ions) from contributing to the conductivity of the solution.[7] Thus, the conductivity of the vesicular solution becomes lower than that of the conductivity of the salt solution.

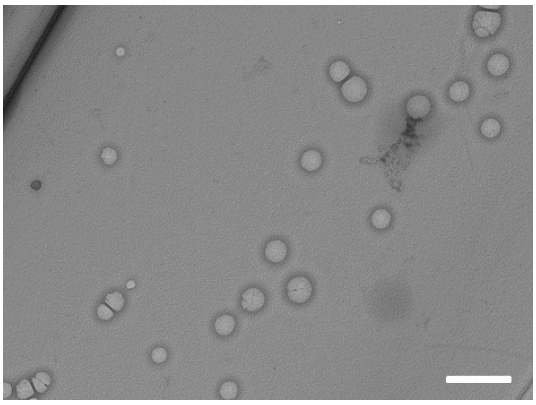

Figure S11. Negative-staining TEM images of DHS solution at concentration of 5 mM which was placed at 25 ^{o}C for one year. Scale bar: 500 nm.

References:

(1) T. Sakai, M. Miyaki, H. Tajima and M. Shimizu, *J.Phys. Chem.B*, **2012**, 116, 11225-11233.

(2) K. S. Rao, P. S. Gehlot, H. Gupta, M. Drechsler and A. Kumar, *J. Phys. Chem. B*, **2015**, 119, 4263-4274.

(3) J. R. Kanicky, A. F. Poniatowski, N. R. Mehta, and D. O. Shah, *Langmuir* **2000**, 16, 172-177.

(4) J. Reijenga, A. Hoof, A. Loon and B. Teunissen, *Anal. Chem. Insights*, **2013**, 8, 53-71.

(5) S. W. Provencher, *Comput. Phys. Commun.*, **1982**, 27, 229-242.

(6) P. Hazra, D. Chakrabarty, A. Chakraborty and N. Sarkar, *Chem. Phys. Lett.*, **2004**, 388, 150-157.

(7) R. Sumita and J. Dey, *Langmuir*, **2005**, 21, 10362-10369.